Terra Antartica
2000, 7(3), 393-400

TERRA ANTARTICA

Preliminary Report on the Main Diagenetic Features of the Oligocene Strata from CRP-2/2A, Victoria Land Basin, Antarctica

F. S. AGHIB[1*], M. CLAPS[2#] & M. SARTI[2]

[1]Dipartimento di Scienze della Terra, Università di Milano, Via Mangiagalli, 34, 20133 Milano - Italy
[2]Istituto Scienze del Mare, Università di Ancona, Via delle Brecce Bianche, 60131 Ancona - Italy
[#]Present address: OKIOC, Raamweg 26, 2596 HL - The Hague - Netherlands

**Corresponding author* (f.aghib@gp.terra.unimi.it)

Received 25 August 1999; *accepted in revised form* 28 April 2000

Abstract - Macroscopic diagenetic features were first recorded and logged in the stratigraphic core description of the CRP-2/2A Initial Report and include carbonate concretions/nodules, carbonate cementation, pyrite and mineral-filled fractures. Fortyfive samples representing the different sedimentary typologies have been selected for further studies on the texture, ultratexture and composition. Authigenic low-Mg calcite is the most common precipitate throughout the core, displaying different main fabric. Fringing cements associated with skeletal fragments and drusy cement within cavities and as vein-infills seem to be related to an early stage of diagenesis. Extensive carbonate cementation occuring below 500 mbsf as blocky calcite crystals is therefore related to a late stage of burial diagenesis as suggested by pressure-solution patterns due to compaction. Authigenic zeolites represent an early stage of diagenesis and are commonly associated with carbonate cementation. Pyrite is mainly present as framboidal void-fillings within biogenic tests and as grains dispersed within the matrix. Silica cementation occurs below 400 mbsf and is more extensive below 500mbsf.

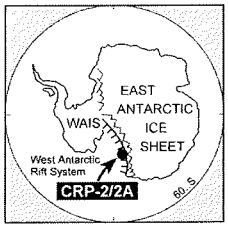

INTRODUCTION

This preliminary study was carried out to evaluate the main diagenetic features of the Oligocene section of the CRP-2/2A core. The CRP-2 drillsite is located 14 km east of Cape Roberts, Ross Sea (Antarctica) at the western margin of the Victoria Land Basin (see Section on Geology). The drilled sequence consists of 624.25 m of glacimarine sediments, spanning in age from Early Oligocene to Plio-Quaternary. The CRP-2/2A core is interpreted to be formed by 24 unconformity-bounded depositional sequences (CRP-2/2A Initial Report; Fielding et al, this issue). The degree of cementation throughout the sequence is highly variable, ranging from poorly indurated lithologies, with cementation restricted to concretions, to well-cemented horizons.

Useful Reports on diagenesis of glacimarine sediments of the Antarctic continental shelf (Ross Sea area) are rare and include Bridle & Robinson on the CIROS-1 core (1990), Baker & Fielding and Claps & Aghib on the CRP-1 core (1998). Several reports from marine/non-marine environments outside the Antarctic region contributed useful information, including Pirrie et al. (1994) and Bailey et al. (1998).

Combined petrographic, sedimentological and compositional investigations of the Oligocene strata from the CRP-2/2A core provide information about the diagenetic environment, the timing of diagenetic events and the nature of the fluid migration. The purpose of this study is an evaluation of the main diagenetic features in order to better understand distinctive diagenetic pathways affecting the drilled sequence.

MATERIALS AND METHODS

Fortyfive samples from the main lithologies and representing different sedimentary types were first impregnated to be prepared for thin sectioning. Textural and sedimentological investigations were performed using a petrographic microscope. Sedimentological observations and compositional analysis were carried out on the same uncovered thin sections using a scanning electron microscope (SEM) attached to an energy dispersive system (EDS). Compositional and ultratextural examinations of the samples were performed mainly at the Eart Science Department of Siena University using a Philips XL30 attached to an EDAX DX4. Few samples were analysed at the Eart Science Department of Milano University using a Cambridge Stereoscan 360. A tentative and preliminary session of SEM coupled with a cathodoluminescence microprobe CL3L was performed on few selected samples from different lithologies in order to identify the subsequent carbonate cement generations within extensive carbonate-cemented lithologies and within calcite vein-infills.

PETROGRAPHY

CARBONATE CEMENTATION ASSOCIATED TO SKELETAL FRAGMENTS

Polychaete worm tubes and other encrusting organims provided with calcitic shells are well preserved and often associated with diffuse carbonate cementation. They are

commonly found in mudstone or very fine sandstone, which appear affected by variable degree of cementation, from poorly to hardly cemented. Polychaete worm tubes are often surrounded by other encrusting organisms with very delicate calcitic shells (Fig. 1: a, b). The skeletal cavities can be at places partially filled by fine sediments similar to the surrounding matrix, but the large remaining voids are filled at a later stage by multiple generations of calcitic cements. First, a fringe of fibrous calcitic cement (crystals 50 μm long) precipitated normally to the shell surface; this is followed by a drusy mosaic of blocky calcitic crystals, increasing in size from the outer part of the cavity towards the centre, and from 100 to 500 μm in size (Fig. 1: b). In the outer part of the shell a thin calcitic layer surrounding the entire skeletal fragment is always present.

CARBONATE-CEMENTED SANDSTONES

The major effect of carbonate cementation is visible on sandy lithologies. Sandstones range from well sorted to very poorly sorted and are very fine- to medium-grained. On a macroscopic scale, carbonate cementation occurs as micro- and macro-nodules, sometimes of irregular shape (from a few mm up to 2-4 cm in diameter, Fig. 3: a). In the growth process they tend to coalesce producing cemented layers of variable thickness along the core, which are mostly responsible the increase in lithification with depth (Fig. 4: a).

Compositionally, these sandstones are dominated by detrital quartz (with grain shape varying from well rounded to angular). Other quartz grains appear intensively fractured (Fig. 4: b). Plagioclase and K-feldspar (microcline) sand grains are common. Dolerite, basalt and granite are the dominant lithologies of rock fragments. Pyroxene, hornblende, olivine and garnet occur as subordinated detrital grains.

The thin section investigation reveals that carbonate cement is competing with terrigenous mud: in the areas where porosity permits the circulation of fluids carbonate cementation takes place. Well rounded quartz grains can be surrounded by a thin dark brownish coating of limited thickness, probably rich in Fe oxide, which may help in reducing the sandstone permeability. In few cases, an authigenic overgrowth of silica cement on detrital quartz grains occurs (Fig. 4: d), outlined by a thin layer of iron oxides. This first layer, when present, is followed by calcite crystals precipitation.

Carbonate precipitation is characterized by a palisade of fibrous calcitic cement (around 10 μm in thickness, Fig. 4: c), while the remainder of the original pore space is filled by a mosaic of equant blocky calcite crystals. The boundary between areas of carbonate cementation and the surrounding sandstone is always quite sharp (Fig.3: c).

MINERAL FILLS IN VEINS AND FRACTURES

Veins have commonly a branching geometry and develop both horizontally and vertically, having a width comprised between less than 1 mm and 0.5 cm . These are filled by two generations of calcitic cement: first a continuous rim of fibrous crystals (20-30 μm in size), which is followed by a late stage of blocky crystals growth (Fig. 2: g). Fractures are present throughout the lower portion of CRP-2A. Often the outer part of their infilling is characterized by fragments of grains or of the lithified host rock enclosed in an early cemented fringe, testifying the active shearing of the fracture during the precipitation of the cement (Fig. 2:h). The inner part show often repeated layers of calcite needle-shaped crystals which are alternated with aligned framboids of pyrite (often in close association with organic matter) or with thin linings of authigenic clay minerals (smectite?). The final phase of cementation is always represented by precipitation of blocky calcite crystals.

DIAGENETIC FEATURES

CARBONATE CEMENTATION ASSOCIATED TO SKELETAL FRAGMENTS

Carbonate cementation in patches, nodules and/or horizons occurs throughout the core below a depth of 150 mbsf and become more intense below 400 mbsf (CRP-2/2A Initial Report). Carbonate cements are the most diverse and volumetrically significant cement present, with several morphologically distinctive types. Compositional analysis revealed that carbonate cement mainly consists of low-Mg calcite showing different main fabric.

Large calcareous biogenic tests as polychaete worm tubes, encrusting organisms, bivalves and gastropods have been recorded at different depths throughout the core (CRP-2/2A Initial Report). Well preserved examples were found in mudstones: these show the original shell, whereas they are in part selectively dissolved in porous lithologies, displaying etches and incipient cementation.

Within fine lithologies (mudstones), the original shells are usually well-preserved and incipient dissolution is present in small areas. Large interlocking crystals of calcite (drusy calcite) are present within the cavities of biogenic tests (Fig. 1: c).

Poorly carbonate-cemented lithologies show "patchy" and irregular calcite rims around grains (mainly quartz, and -to a lesser extent- feldspars, plagioclase, rock fragments) (Fig. 1: d, e).

Calcareous microfossils have not been observed, whereas well-preserved siliceous tests have been recorded within the carbonate-cemented patches (Fig. 1: f). Below 400 mbsf siliceous microfossils are mostly crushed due to compaction.

Extensive cementation occurs below 400 mbsf. The strongly-carbonate-cemented lithologies show a late syntaxial growth of low-Mg calcite around grains (Fig. 2: a, b). The main fabric is composed by equant, blocky and euhedral crystals of calcite which is interpreted as a late stage of cementation. Pressure-solution patterns have been recorded on grains of quartz and are due to compactional effects (Fig. 2: a, b, c, d)

Low Mg-calcite around grains occurs as early diagenetic carbonate-cement associated with skeletal fragments, as well as late extensive burial cement. No Mg-

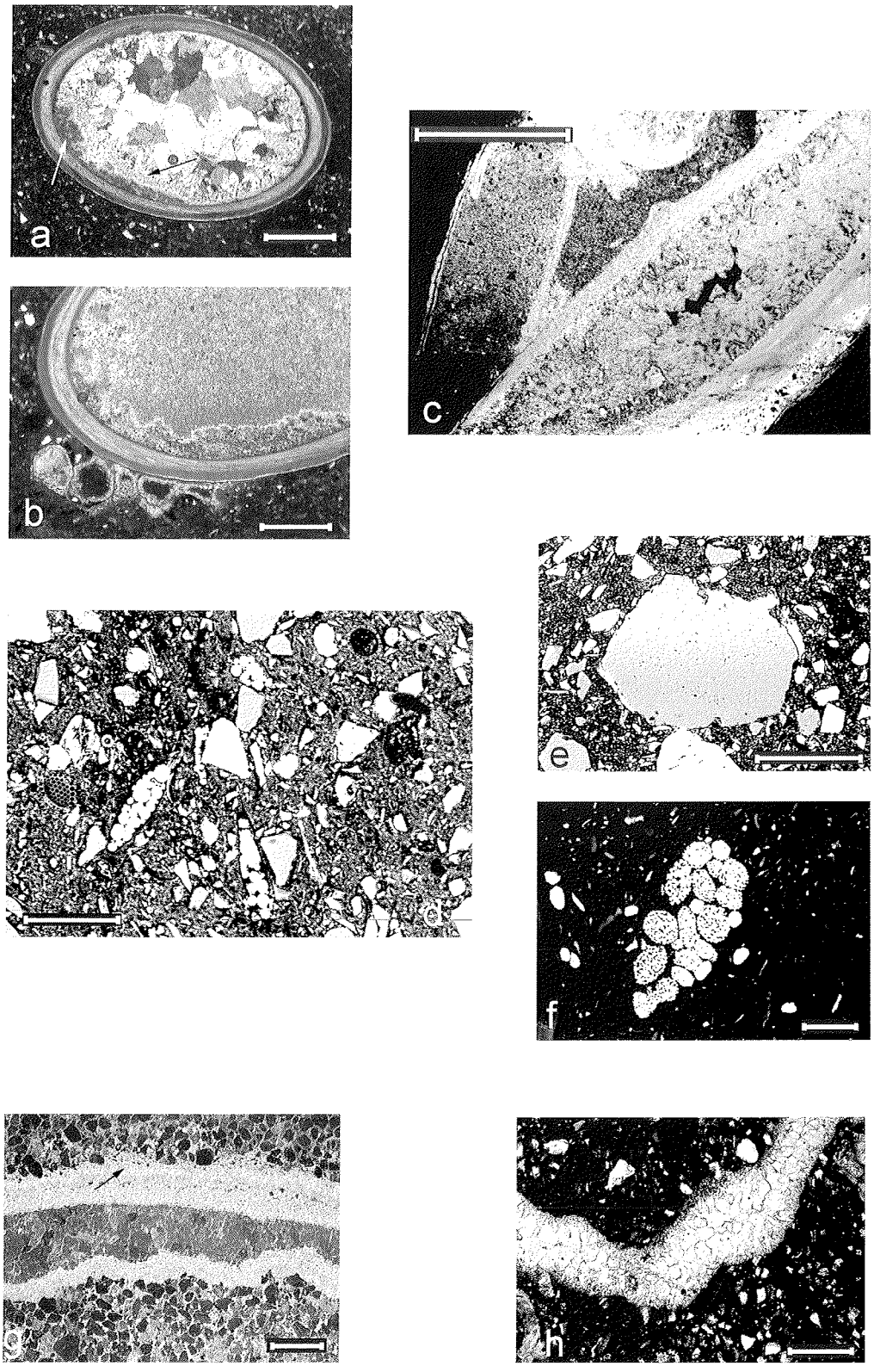

Fig.1 - Early low-Mg calcite cements, calcite vein-fills and framboidal pyrite.
a) Inner cavity of a polychaete worm tube with areas occupied by terrigenous mud (white arrow), then filled by two generations of cement (342.07 mbsf; scale bar 500 μm): the thin fringe of fibrous calcitic cement (black arrow) is followed by a drusy mosaic of calcite blocky crystals; b) Polychaete worm tube with its multilayer test still preserved (342.07 mbsf; scale bar 500 μm); other encrusting organisms are surrounding the worm tube; c) Large serpulid showing the well-preserved original shell; incipient dissolution on the smaller encrusting test (top left). Drusy calcite composed of large interlocking crystals of low-Mg calcite. Tiny framboids of pyrite lining the inner wall (341.87 mbsf; scale bar 2 mm); d) Well preserved siliceous biogenic tests (mainly diatoms) within a fine-grained poorly–cemented matrix. Note framboidal pyrite as void-fillings (450.68 mbsf; scale bar 100 μm); e) Incipient cementation by low-Mg calcite around quartz grains in poorly–cemented fine lithologies (187.40 mbsf; scale bar 200 μm); f) Framboids of pyrite as void-fillings within a diatom test (565.70 mbsf; scale bar 20 μm); g) Fracture filled by a first generation of fibrous calcitic crystals, which enclose small fragments of the host rock (black arrow). The remainder of the fracture is sutured by equant calcite (596.67 mbsf; scale bar 1 mm); h) Thin vein occurring in sandy mudstone (97.34 mbsf; scale bar 500 μm). The open cavity is filled by two generations of calcitic cement: first a continuos rim of fibrous crystals, then followed by a late stage of blocky crystals growth.

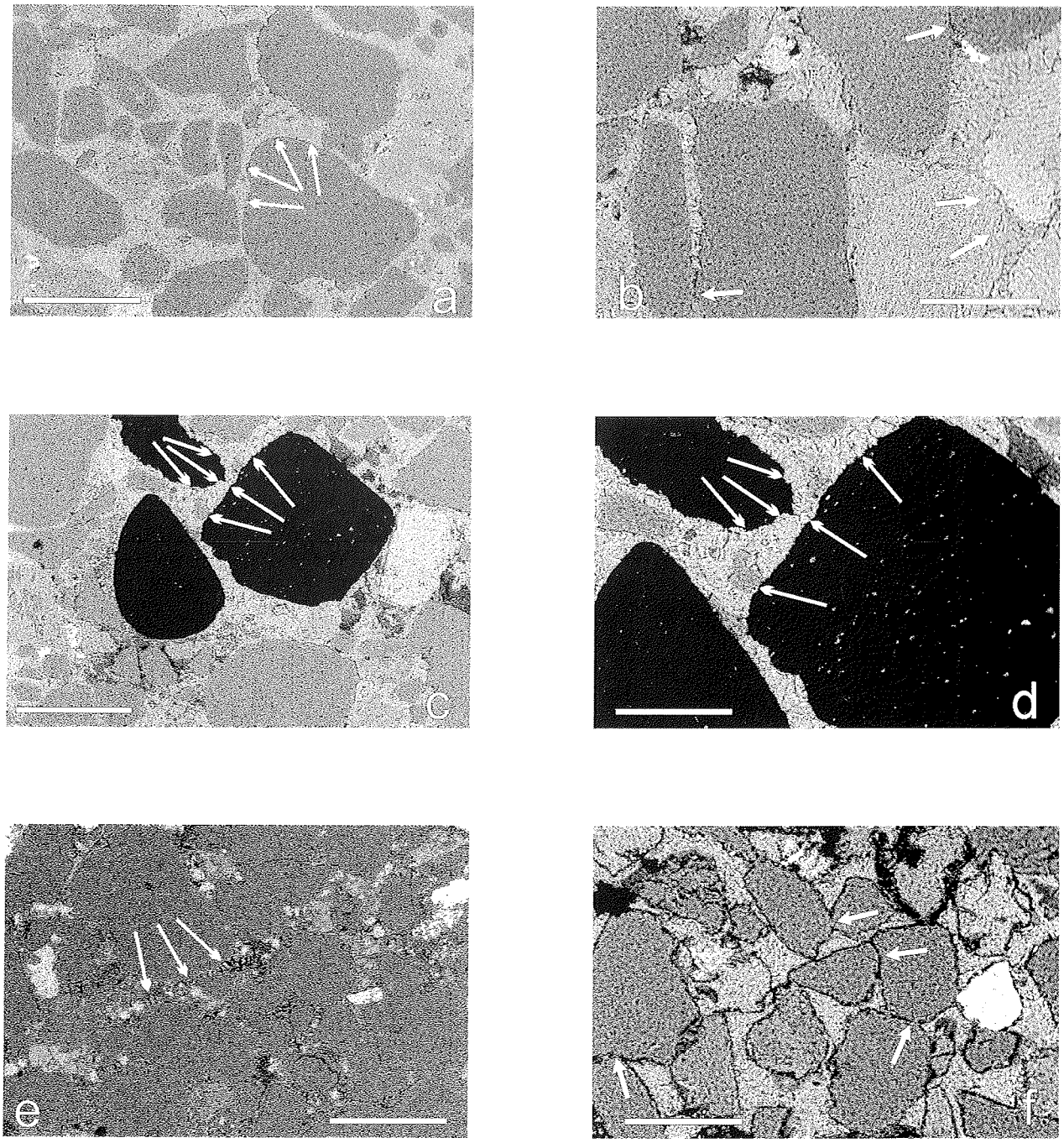

Fig. 2 - Ultratexture of low-Mg calcite cements and Ultratexture of silica cements.
a) and b) Ultratexture of late low-Mg calcite: large euhedral crystals along grains, after compaction effects (arrows; a: 423.88 mbsf; scale bar 200 μm; b: 423.88 mbsf; scale bar 100 μm); c) and d) Ultratexture of low-Mg calcite: syntaxial crystal growth along grains (c: 423.88 mbsf; scale bar 200 μm; d: 423.88 mbsf; scale bar 100 μm); e) Ultratexture of silica cements: palisade crystals around grains (618.86 mbsf; scale bar 200 μm); f) Ultratexture of silica cements: late pervasive and blocky cementation. Note pressure-solution patterns along quartz grains (arrows; 502.12 mbsf; scale bar 100 μm).

calcite, no iron –rich calcite and no siderite microconcretions have been observed. Zeolites and tiny rhombs of ankerite minerals were observed within the extensive carbonate-cemented lithologies and they are interpreted as authigenic minerals related to an early stage of diagenesis.

Cathodoluminescence analysis on samples below 450-500 mbsf confirmed that the Mg-calcite blocky cement is composed of a single generation of non-luminescent cement (probably) related to a late stage of diagenesis.

CARBONATE-CEMENTED SANDSTONES

Millimetric and centimetric carbonate-cemented nodules were recorded in sandstone lithologies below 500 mbsf (Fig. 3: a; Fig. 4: a). Scanning electron microscopy revealed that the porous and poorly carbonate-cemented areas surrounding the nodules are mostly composed of quartz grains and do not show any cementation (Fig. 3: d). Tiny zeolite crystals have been observed lining the grains (see arrows, in Fig. 3: e, f).

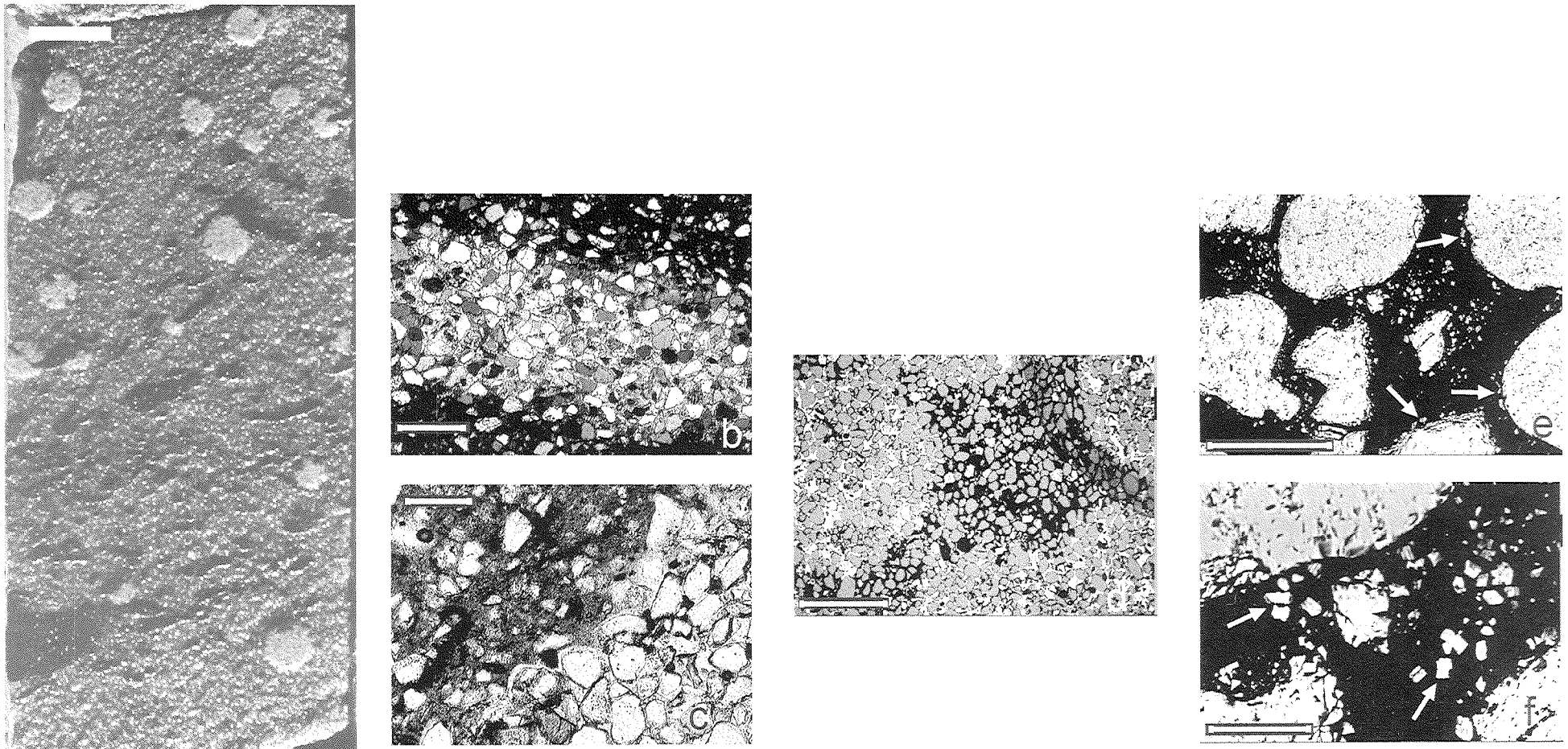

Fig. 3 - Texture and ultratexture of the carbonate-cemented sandstones; a) Working half of the core at 516.00 mbsf showing carbonate micro-nodules in fine to medium sandstone (scale bar 1 cm); b) Elongated carbonate cemented micro-nodule in very fine and fine sandstone, showing the sharp boundary between cement and terrigenous mud (in black). Grains are commonly quartz and plagioclase (scale bar 500 μm); c) Sharp boundary between carbonate cemented and uncemented medium-grained sandstone (556.79 mbsf; scale bar 200 μm); d) Millimetric carbonate-cemented nodules (clear areas are carbonate-cemented) within non-cemented sands (573.49 mbsf; scale bar 2 mm); e) Ultratexture of non-cemented sands. Subrounded quarz grains showing no cementation. Note small zeolite crystals (arrows) lining quartz grains (573.49 mbsf; scale bar 200 μm); f) Ultratexture of non-cemented sands. Note small zeolite crystals (arrows) lining quartz grains (573.49 mbsf; scale bar 50 μm).

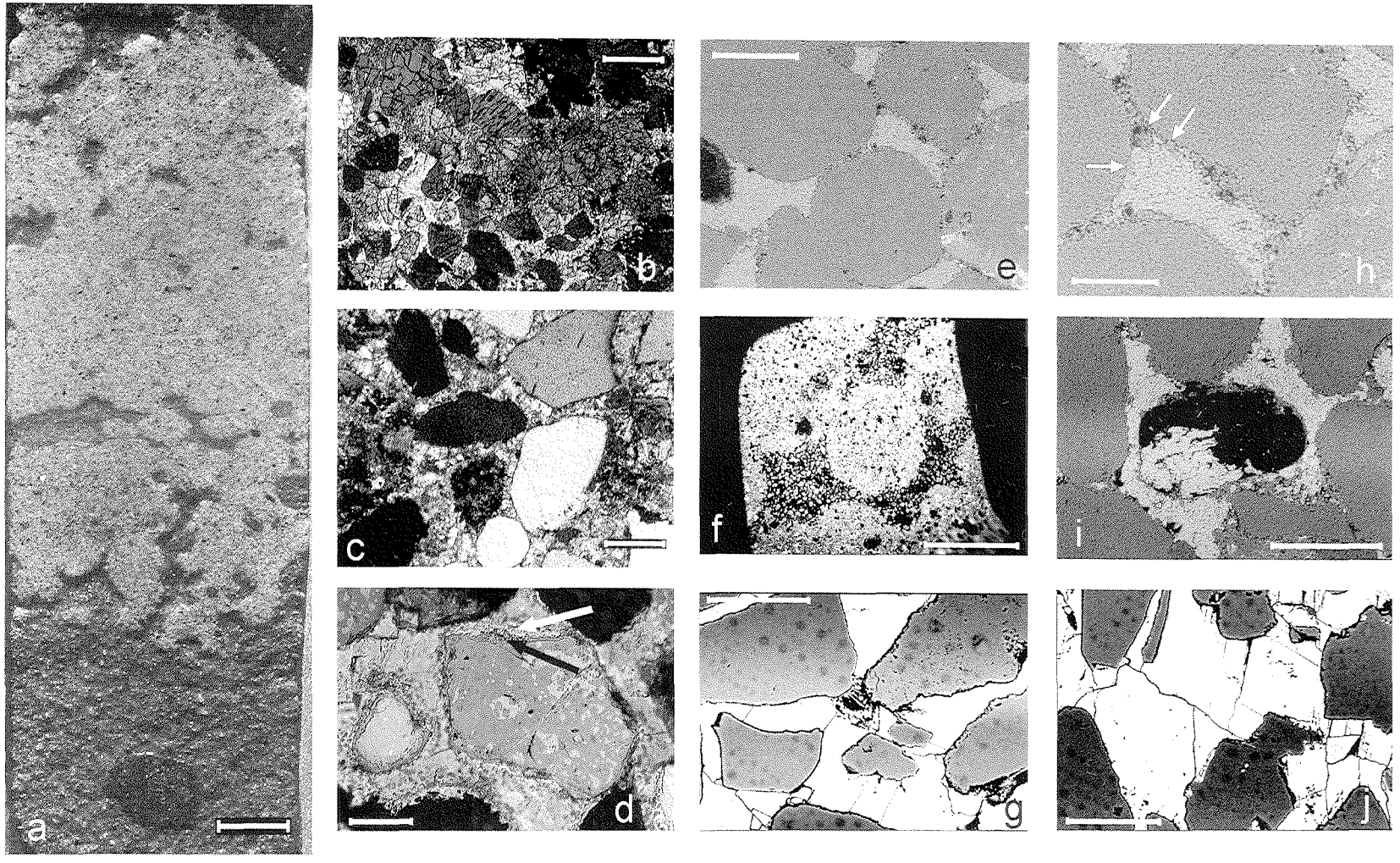

Fig. 4 - Texture and ultratexture of the carbonate-cemented sandstones.
a) Working half of the core at 525.36 mbsf showing the massive carbonate cemented sandstone as result of the micro-nodules coalescence (scale bar 1 cm); b) Detrital quartz grains, highly fractured, enclosed in a mosaic of calcitic cement (556.79 mbsf; scale bar 200 μm); c) Palisade of fibrous calcitic crystals cementing quartz grains (618.86 mbsf; scale bar 100μm); d) Authigenic overgrowth of silica cement in optical continuity on a quartz grain (black arrow), followed by a thin fringe of fibrous calcite (white arrow). The pore space has been definitively filled by calcite precipitation (573.49 mbsf; scale bar 100 μm); e) Ultratexture of the carbonate-cemented sandstones showing quartz grains, zeolites and pervasive low-Mg calcite cementation (554.46 mbsf; scale bar 100 μm); f) Texture of carbonate-cemented sandstones. Nodules are well recognizible. (573.49 mbsf; scale bar 5 mm); g) Rhombohedral (probably ankerite) microconcretion crushed by quartz grains. Note extensive cementation (556.79 mbsf; scale bar 100 μm); h) Close-up of e): blocky ultratexture of the equant crystals of low-Mg calcite, arrows indicate zeolites (554.46 mbsf; scale bar 50 μm); i) Pervasive low-Mg calcite cementation around quartz grains and within coal grains (589.30 mbsf; scale bar 200 μm); j) Close-up of g): blocky ultratexture of the equant crystals of low-Mg calcite (556.79 mbsf; scale bar 100 μm).

Scanning electron microscopy observations on the carbonate-cemented nodules have shown that the cement is composed of low-Mg and low-Fe calcite and shows a blocky texture and equant crystal shapes (Fig. 4: e, f). Rhombohedral (probably ankerite) microconcretions (50 μm in size) are common within carbonate-cemented nodules and seem to be crushed by the surronding grains (Fig. 4: g). The microconcretions are composed of several layers of Fe-rich and Mg-rich carbonate, and each layer differs in Fe content. Small zeolite crystals (5 μm in size) occur within the cement and within the microconcretions of ankerite (Fig. 4: h).

Pressure solution features due to compaction effects occur along the grains (Fig. 4: e, h, i).

In a few samples calcitic cementation occurs within detrital grains of coal particles which seem to be partly consumed, suggesting a carbon-carbonate diagenesis (Fig. 4: i; Lamothe et al. 1983).

The main fabric of the carbonate-cemented nodules suggests that growth of the zeolite crystals and subsequent formation of the microconcretions occur during an early stage of diagenesis. The initial compaction may have reduced porosity considerably and broken the fragile ankerite microconcretions. No internal textures have been observed in any of the investigated samples. The remarkably equant and blocky fabric of the calcitic cement is therefore interpreted as an extensive and late stage cementation related to burial diagenesis. Cathodoluminescence investigations on the calcitic cement confirmed that it is composed by a single generation of non-luminescent calcite (low-Mg, low-Sr). C, O isotopes might clarify the origin of the extensive carbonate cementation.

PYRITE

Tiny crystals (5-50 μm) of pyrite are common throughout the core in a range of morphologies. Framboidal pyrite is present as discrete grains dispersed within the matrix in fine lithologies and as void-fillings within biogenic tests (especially diatoms, Fig. 1: f). Pyrite is also found in association with carbonate cements infilling original porosity in biogenic tests (Fig. 1: c). Moreover, a few occurrences of pyrite as discrete cement phase, associated with volcanoclastic material, have been observed in sandy lithologies.

SILICA CEMENTATION

Silica cementation occurs in association with compactional effects such as crushing and pressure-solution features between quartz grains and suggests that silica precipitation is related to a burial diagenesis. A late stage silica cementation has been recorded as euhedral palisade crystals around grains only below a depth of 400 mbsf (Fig. 2: e, f) and as an extensive cementation showing a blocky ultratexture below 500 mbsf. Sparse silica cements have been also recorded in the upper 300 metres of the drilled sequence (van der Meer, pers. comm.).

MINERAL- FILLS IN VEINS AND FRACTURES

Scanning electron microscopy observations allow us to recognize mineral-fills occurring along faults and in veins. Mineral–fills are composed of low-Mg calcite and show diffusion within the porous host lithologies. They seem to be composed of different generations of cements. Individual calcite crystals are up to 0.5 cm long. Calcite shows a dull- to non-luminescence under cathodoluminescence. Mineral-fills along faults are characterized by fragments of the host rock trapped within the cement which consists of different generations of low-Mg calcite showing a thin lining of pyrite cement precipitate.

DISCUSSION

Although the factors controlling the diagenesis are well-known in most environments, glacimarine areas are less investigated. Several investigations have explored the possibility to use geochemistry of carbonates from glacial sediments as clues to palaeoenvironmental interpretation (Eyles et al., 1985; Fairchild et al., 1988; Fairchild & Spiro, 1990). These papers investigated the origin of glacial carbonates from different settings (detrital carbonates, subglacial precipitates, skeletal carbonates, diagenetic carbonates) but few have combined a petrographic and a geochemical approach.

The diagenesis affecting the CRP-2/2A sediments is not simply burial-dependent, but is related to several cycles of glacial advance/retreat over the drillsite. Therefore the nature of the fluid migration within porous lithologies and along fractures and faults might be the controlling factor of the main diagenetic features *i.e.* extensive carbonate cementation, precipitation of authigenic minerals such as calcite, carbonates, pyrite, zeolites within the matrix and as vein infills. The burial diagenesis seems to affect the deeper strata in terms of texture and ultratexture (fabric, compactional effects such as crushing, pressure-solution patterns).

Textural, ultratextural and compositional investigations of the carbonate cements allow a tentative paragenesis of the Oligocene strata to be inferred. 1) an early diagenetic and shallow burial fringing low-Mg calcite cement associated with skeletal material; 2) an early drusy and sparry low-Mg calcite cement; 3) a late blocky low-Mg calcite cement.

On the basis of textural evidences, fringing cements are the earliest diagenetic carbonates. As reported by Baker & Fielding and Claps & Aghib for the CRP-1 precipitation of low-Mg calcite might be related to dissolution of poorly stable aragonitic and/or Mg-calcite biogenic tests and precipitation of stable low-Mg calcite as fringing cements. Drusy low-Mg calcite cement within biogenic tests and as infills in veins are considered to represent relatively early diagenetic cement precipitates prior to significant compaction of the sedimentary sequence. They are therefore related to an early stage of

burial diagenesis. Blocky calcite texture might represent the post-compactional and late stage carbonate cementation, as suggested by the breakage of grains and the pressure-solution features occurring along grains. The carbonate-cemented nodular sandstones represent all stages of a late and extensive cementation: from sparse centimetric carbonate-cemented nodules within coarse sandy lithologies to well-cemented sandstones. The occurrence of carbonate cementation within coal fragments may suggest that their formation is related to organic carbon-carbonate diagenesis, as previously recorded in glacio-lacustrino/glacimarine environments (Lamothe et al, 1983).

The diagenetic minerals recorded throughout the CRP-2/2A core are directly comparable to those previously described for other glacimarine sedimentary sequences recovered in the Ross Sea area at CIROS-1 (Bridle & Robinson, 1990) and at CRP-1 drillsites (Baker & Fielding and Claps & Aghib, 1998) and also to those previously reported for other environments (Pirrie et al., 1994, Bailey et al., 1998). In the CRP-2 sedimentary sequence, the early diagenetic phases are controlled by pore water conditions. The framboidal pyrite is related to bacterial sulphate reduction at very shallow burial depth (Berner, 1984 and further works summarized in Morse et al., 1987). Pyrite formation can be interpreted as carbon sourced from the breakdown of organic matter during sulfate reduction related to marine porewaters. The distribution of calcitic cements associated with skeletal fragments was controlled by dissolution of biogenic tests. The early diagenetic fringing cements in the carbonate-cemented sandstones may be formed at shallow burial depth. Subsequent extensive cements in these lithologies were precipitated in a late stage, and the original early (fringing) cements were at least partially recrystallized. Late stage burial cements are mainly associated with dewatering as a result of overpressuring.

In core CRP-2/2A, zeolites have been recorded also in poorly-lithified sandy lithologies and are interpreted as an early diagenetic precipitates as previously recorded in the CIROS-1 core by Bridle & Robinson (1990). Microconcretions of ankerite are present mainly in sandstones. Variations in Mg/Fe contents within a concretion are random and suggest fluctuations during their formation. Their formation seems to be related to low-salinity porewaters (meteoric?) and bacterial activity may have influenced their compositions (Mortimer et al., 1997).

ACKNOWLEDGEMENTS

Professor C. A. Ricci (Siena University) kindly made available Philips XL30 scanning electron microscope at his institution and G. Giorgetti provided valuable technical assistance and scientific support. Professor P. Barrett, Dr. C. Fielding and the CRP team are thanked for critical and useful suggestions during the CRP-2 drilling season. Professor M. B. Cita contributed helpful discussions. C. Malinverno prepared several thin sections. A. Rizzi helped in taking micrographs at University of Milano. This study is financially supported by a PNRA/CRP research grant.

REFERENCES

Cape Roberts Science Team, 1998a. Background to CRP-1, Cape Roberts Project, Antarctica. *Terra Antartica*, **5**(1), 1-30.

Cape Roberts Science Team, 1998b. Quaternary Strata in CRP-1, Cape Roberts Project, Antarctica. *Terra Antartica*, **5**(1), 31-61.

Cape Roberts Science Team, 1998c. Miocene Strata in CRP-1, Cape Roberts Project, Antarctica. *Terra Antartica*, **5**(1), 63-124.

Cape Roberts Science Team, 1998d. Summary of Results from CRP-1, Cape Roberts Project, Antarctica. *Terra Antartica*, **5**(1), 125-137.

Cape Roberts Science Team, 1999. Initial Report on CRP-2/2A, Cape Roberts Project, Antarctica. *Terra Antartica*, **6**(1/2), 1-173.

Bailey A. M., Roberts H. H. & Blackson J. H., 1998. Early diagenetic minerals and variables influencing their distributions in two long cores (>40 m), Missisipi River Delta Plain. *Journal of Sedimentary Research*, **68**(1), 185-197.

Baker J.C. & Fielding C.R., 1998. Diagenesis of Glacimarine Miocene Strata in CRP-1, Antarctica. *Terra Antartica*, **5**(3), 647-653.

Berner R.A., 1984. Sedimentary pyrite formation: An update. *Geochimica et Cosmochimica Acta*, **48**, 605-615.

Bridle I. M. & Robinson P. A., 1990. Diagenesis. In: Barrett P. J. (ed.), *Antarctic Cenozoic history from the CIROS-1 drillhole McMurdo Sound. DSIR Bulletin*, **245**, 201-207.

Claps M. & Aghib F.S., 1998. Carbonate Diagenesis in Miocene Sediments from CRP-1, Victoria Land Basin, Antarctica. *Terra Antartica*, **5**(3), 655-660.

Eyles C. H., Eyles N. & Miall A. D., 1985. Models of glacimarine sedimentation and their application to the interpretation of ancient glacial sequences. *Palaeogeography, Palaeoclimatology, Palaeoecology, **51**, 15-84.*

Fairchild I.J, Hendry G.L., Quest M. & Tucker M.E., 1988. Chemical analysis of sedimentary rocks. In: Tucker M. E. (ed), *Techniques in Sedimentology*. Blackwell, Oxford, 271-352.

Fairchild I.J. & Spiro B., 1990. Carbonate minerals in glacial sediments:geochemical clues to palaeoenvironment. In: Dowdeswell J. A. & Scourse J. D. (eds), *Glacimarine Environments: Processes and Sediments, Geological Society Special Publication*, **53**, 201-216.

Lamothe M., Hillaire-Marcel C. & Page P., 1983. Decouverte de concretions calcaires dans le till de Gentilly, basses-terres du Saint-Laurent, Quebec. *Canadian Journal of Earth Sciences*, **20**, 500-505.

Morse J. W., Millero F. J., Cornwall J. C. & Rickard D., 1987. The chemistry of hydrogen sulfide and iron sulfide systems in natural waters. *Earth-Science Reviews*, **24**, 1-42.

Mortimer R.J.G., Coleman M.L. & Rae J.E., 1997. Effect of bacteria on the elemental composition of early diagenetic siderite: implications for paleoenvironmental interpretations. *Sedimentology*, **44**, 759-765.

Pirrie D., Ditchfield P.W. & Marshall J.D., 1994. Burial diagenesis and pore-fluid evolution in Mesozoic back-arc basin: the Marambio Group, Vega Island, Antarctica. *Journal of Sedimentary Petrology*, **64**(3), 541-552.